

Competing Reaction Mechanisms for the Carbonylation of Neutral Palladium(II) Complexes Containing Bidentate Ligands: A Theoretical Study

Katrina E. Frankcombe, Kingsley J. Cavell, and Brian F. Yates*

Department of Chemistry, University of Tasmania, GPO Box 252-75,
Hobart 7001, Tasmania, Australia

Robert B. Knott

Australian Nuclear Science and Technology Organization, Private Mail Bag 1,
MENAI, New South Wales 2234, Australia

Received January 29, 1997[®]

The complete carbonylation mechanism for the model palladium(II) system, $\text{Pd}(\text{PH}_3)(\text{CH}_3)(\text{N}-\text{O}) + \text{CO} \rightarrow \text{Pd}(\text{PH}_3)(\text{COCH}_3)(\text{N}-\text{O})$ ($\text{N}-\text{O} = \text{NHCHCOO}^-$), has been investigated employing nonlocal density functional theory (DFT) and second-order Møller–Plesset perturbation theory (MP2). Four possible mechanisms were identified, all involving the initial displacement of the phosphine ligand by carbon monoxide *via* a trigonal bipyramidal transition structure. Of these four mechanisms, the rate-determining methyl migration step was found to be lowest in energy when proceeding from a novel five-coordinate intermediate in which the palladium–nitrogen bond is weakened (2.385 Å at the MP2 level of theory). This mechanism is consistent with the available experimental data. MP2 calculations using large basis sets predicted an overall exothermicity of -59.7 kJ/mol and a negligible activation energy of $+6.0$ kJ/mol with respect to the separated reactants. In addition, a novel transition structure that accounts for the isomerization of square-pyramidal d^8 complexes is presented.

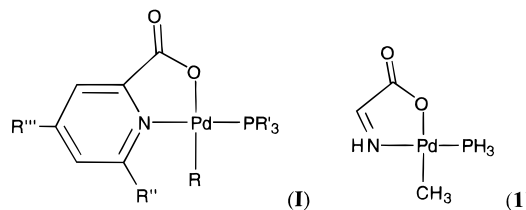
Introduction

Carbonylation reactions utilizing palladium(II) complexes are of increasing importance, particularly in view of developments in the CO/ethylene copolymerization process to form polyketones.^{1–4} With the rapid advances in computational techniques, the use of theoretical modeling is becoming a valuable tool in the design of new catalysts, enhancing the traditional experimental methods, and resolving mechanistic steps which purely experimental approaches have been unable to elucidate.^{5,6} The use of palladium(II) chelate complexes as catalysts is of particular and current interest.^{7–10}

Experimental and theoretical evidence indicates that the so-called carbonyl insertion step proceeds with few exceptions¹¹ *via* migration of the alkyl group to the coordinated CO ligand, rather than by insertion of CO into the palladium–alkyl bond.¹² There has been

considerable debate concerning how carbonylation takes place when the carbon monoxide is not initially coordinated to the metal.^{8,13,14} It has been proposed that it may occur directly from a five-coordinate species or from a four-coordinate species following ligand displacement.¹³ *Ab initio* calculations performed by Markies *et al.*¹⁵ on the model systems $\text{Pd}(\text{NH}_3)_3(\text{CH}_3)^+$ and $\text{Pd}(\text{NH}_3)_2(\text{CH}_3)_2$ indicated that carbon monoxide displaces one of the NH_3 groups to yield a four-coordinate complex from which migration could proceed. Although the results precluded the formation of strongly bound five-coordinate intermediates, the transition structure for methyl migration in the cationic species was found to be stabilized by the dissociated nitrogen remaining in the vicinity of the coordination sphere.

Recent experimental studies have shown palladium(II)–alkyl complexes of pyridine carboxylic acid derivatives (I) undergo rapid carbonylation.^{10,16,17} From the

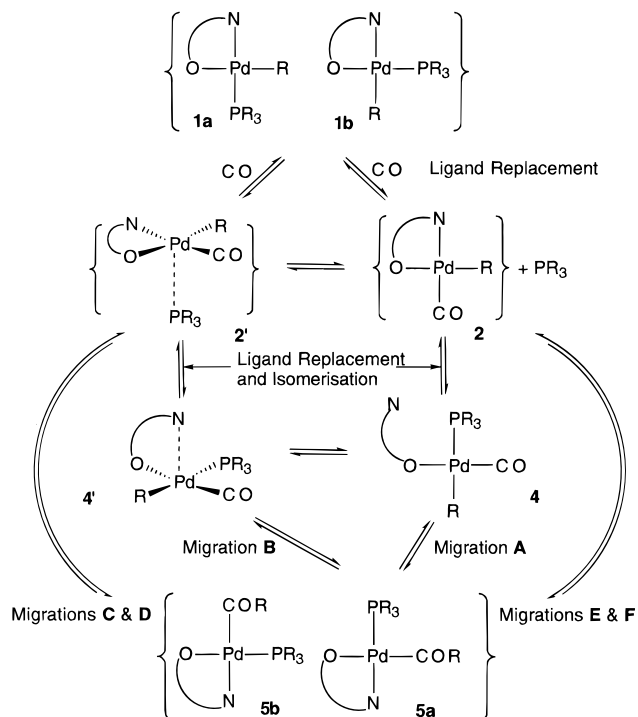


[®] Abstract published in *Advance ACS Abstracts*, May 15, 1997.

- (1) Sen, A. *Acc. Chem. Res.* **1993**, *26*, 303.
- (2) Jiang, Z.; Sen, A. *J. Am. Chem. Soc.* **1995**, *117*, 4455.
- (3) Drent, E.; Arnoldy, P.; Budzelaar, P. H. M. *J. Organomet. Chem.* **1994**, *475*, 57.
- (4) Drent, E.; Budzelaar, P. H. M. *Chem. Rev.* **1996**, *96*, 663.
- (5) Koga, N.; Morokuma, K. *Chem. Rev.* **1991**, *91*, 823.
- (6) Budzelaar, P. H. M.; van Lenthe, J. H. In *Theoretical Aspects of Homogeneous Catalysis: Applications of ab Initio Molecular Orbital Theory*; van Leeuwen, P. W. N. M., Morokuma, K., van Lenthe, J. H., Eds.; Kluwer Academic Publishers: Netherlands, 1995; pp 3–13.
- (7) Dekker, G. P. C. M.; Buijs, A.; Elsevier, C. J.; Vrieze, K.; van Leeuwen, P. W. N. M.; Smeets, W. J. J.; Spek, A. L.; Wang, Y. F.; Stam, C. H. *Organometallics* **1992**, *11*, 1937.
- (8) van Asselt, R.; Gielen, E. E. C. G.; Rülke, R. E.; Vrieze, K.; Elsevier, C. J. *J. Am. Chem. Soc.* **1994**, *116*, 977.
- (9) Markies, B.; Kruis, D.; Rietveld, M. H. P.; Verkerk, K. A. N.; Boersma, J.; Kooijman, H.; Lakin, M. T.; Spek, A. L.; Koten, G. V. J. *Am. Chem. Soc.* **1995**, *117*, 5263.
- (10) Cavell, K. J.; Jin, H.; Skelton, B. W.; White, A. H. *J. Chem. Soc., Dalton Trans.* **1995**, 2159.

- (11) van Leeuwen, P. W. N. M.; Roobeek, C. F.; van der Heijden, H. *J. Am. Chem. Soc.* **1994**, *116*, 12117.
- (12) Koga, N.; Morokuma, K. *J. Am. Chem. Soc.* **1985**, *107*, 7230.
- (13) Anderson, G. K.; Cross, R. J. *Acc. Chem. Res.* **1984**, *17*, 67.
- (14) Blomberg, M. A.; Karlsson, C. A. M.; Siegbahn, P. E. M. *J. Phys. Chem.* **1993**, *97*, 9341.
- (15) Markies, B. A.; Wijkens, P.; Dediou, A.; Boersma, J.; Spek, A.; Vankoten, G. *Organometallics* **1995**, *14*, 5628.

Scheme 1. Proposed Reaction Pathways for the Carbonylation of Neutral Palladium(II)–Alkyl Complexes of Pyridine Carboxylic Acid (pyca)^a



^a Species in parentheses may exist as an isomeric mixture, although, for simplicity, the second isomer is not always shown. Different isomers are distinguished by the letters a and b.

early experimental work,¹⁶ the mechanistic proposals illustrated in Scheme 1 were postulated as possible reaction pathways. These encapsulate the observed importance of the lability of the nitrogen donor and the lability and *trans* influence of the phosphine ligand. Note that an isomeric mixture of the reacting complex is used, but only one isomer of the final acyl complex (N *trans* to P, **5a**) is obtained. In addition, the possibility of direct insertion of uncoordinated carbon monoxide into the metal–methyl bond must not be excluded.

We have previously carried out a theoretical study on the first step in the carbonylation process, the replacement of phosphine by carbon monoxide in Pd(CH₃)(PH₃)(N–O) (N–O = NHCHCOO[−]) (**1**) for the *trans*(N,P) isomer (Figure 1) to establish a theoretical method appropriate for the study of such systems.¹⁸ MP2 calculations with large basis sets indicated that carbon monoxide initially binds weakly to the metal center to form a flattened square-pyramidal structure **1'a**. This complex was found to be stabilized by 18.8 kJ/mol with respect to the separated species. Ligand substitution proceeds *via* a trigonal-bipyramidal transition structure with a barrier of +14.3 kJ/mol relative to **1'a**. Once “displaced”, the phosphine remains weakly bound to the metal, forming a flattened square-pyramidal five-coordinate complex **2'a** with an energy of −22.2 kJ/mol with respect to the separated reactants. We concluded that it appears unlikely that the phosphine would fully dissociate to form **2** + PH₃; moreover, the subsequent transformations would proceed directly from **2'a**.¹⁸

In the present study, we present a theoretical investigation of each of the possible mechanisms outlined in Scheme 1, allowing us to predict the dominant pathways and rate-determining steps for the carbonylation reaction. To make the computations tractable, we have simplified the experimental system (**1**) to the model system (**1**). For qualitative purposes, this system is not far removed from the experimental one; the model chelate ligand retains the backbone of pyridine carboxylate (pyca), including some delocalization effects and the π -accepting ability of the nitrogen donor. Although inadequacies exist in the use of PH₃ to model triphenylphosphine, it remains useful for qualitative discussions.^{19,20} To our knowledge, this study represents the first investigation of the carbonylation of palladium(II) complexes containing hemilabile chelate ligands. In addition, we provide new and tangible evidence for the participation of five-coordinate intermediates and transition structures in the fundamental transformations of d⁸ palladium complexes.

Computational Methods

The calculations were performed using GAUSSIAN 92 version F (which includes the DFT package)²¹ and GAUSSIAN 94, revision B.3,²² on Sun sparc 690 workstations and Fujitsu VP2200/10 and CRAY J90 high-performance computers.

Full geometry optimizations were carried out using gradient optimization. Transition structures were located using the eigenvector-following optimization method which updates the Hessian at each step of the optimization.^{23,24} The potential energy surface (PES) was followed “downhill” by gradient optimization on either side of the saddle point to the intermediates.

The PES was initially probed at the RHF level of theory using the large-core relativistic effective core potential (RECP) of Hay and Wadt.²⁵ The corresponding minimal valence basis set (3s/3p/4d)/[3/3/4]²⁵ was used for the metal valence and STO-3G on the main group elements. The geometries and force constants calculated at this level of theory were used as starting points for high-level calculations. As analytical second derivatives for RECPs were not available to us, frequency calculations were performed only at this level of theory. These calculations confirmed the correct nature of each of the stationary points on the PES.

Improved geometries were obtained using gradient-corrected DFT and, in some cases, MP2 methods. The small-core RECP of Hay and Wadt (denoted LANL2) was employed for the metal with the (8s/6p/4d)/[341/321/31] contraction for the valence region which includes the 4s and 4p orbitals.²⁶ The 6-31G(d) basis set was adopted for the main group elements. This

(18) Frankcombe, K. E.; Cavell, K. J.; Yates, B. F.; Knott, R. B. *J. Phys. Chem.* **1996**, *100*, 18363.

(19) Häberlen, O. D.; Rösch, N. *J. Phys. Chem.* **1993**, *97*, 4970.

(20) Sargent, A. L.; Hall, M. B. *Inorg. Chem.* **1992**, *31*, 317.

(21) Frisch, M. J.; Trucks, G. W.; Head-Gordon, M.; Gill, P. M. W.; Wong, M. W.; Foresman, J. B.; Johnson, B. G.; Schlegel, H. B.; Robb, M. A.; Replogle, E. S.; Gomperts, R.; Andres, J. L.; Raghavachari, K.; Binkley, J. S.; Gonzalez, C.; Martin, R. L.; Fox, D. J.; Defrees, D. J.; Baker, J.; Stewart, J. J. P.; Pople, J. A. *GAUSSIAN 92*; Gaussian, Inc.: Pittsburgh, PA, 1992.

(22) Frisch, M. J.; Trucks, G. W.; Schlegel, H. B.; Gill, P. M. W.; Johnson, B. G.; Robb, M. A.; Cheeseman, J. R.; Keith, T.; Peterson, G. A.; Montgomery, J. A.; Raghavachari, K.; Al-Laham, M. A.; Zakrzewski, V. G.; Ortiz, J. V.; Foresman, J. B.; Peng, C. Y.; Ayala, P. Y.; Chen, W.; Wong, M. W.; Andres, J. L.; Replogle, E. S.; Gomperts, R.; Martin, R. L.; Fox, D. J.; Binkley, J. S.; Defrees, D. J.; Baker, J.; Stewart, J. P.; Head-Gordon, M.; Gonzalez, C.; Pople, J. A. *GAUSSIAN 94*; Gaussian, Inc.: Pittsburgh, PA, 1995.

(23) Baker, J. *J. Comput. Chem.* **1986**, *7*, 385.

(24) Baker, J. *J. Comput. Chem.* **1987**, *8*, 563.

(25) Hay, P. J.; Wadt, W. R. *J. Chem. Phys.* **1985**, *82*, 270.

(26) Hay, P. J.; Wadt, W. R. *J. Chem. Phys.* **1985**, *82*, 299.

(16) Jin, H.; Cavell, K. J. *J. Chem. Soc., Dalton Trans.* **1994**, 415.

(17) Hoare, J. L.; Cavell, K. J.; Hecker, R.; Skelton, B. W.; White, A. H. *J. Chem. Soc., Dalton Trans.* **1996**, 2197.

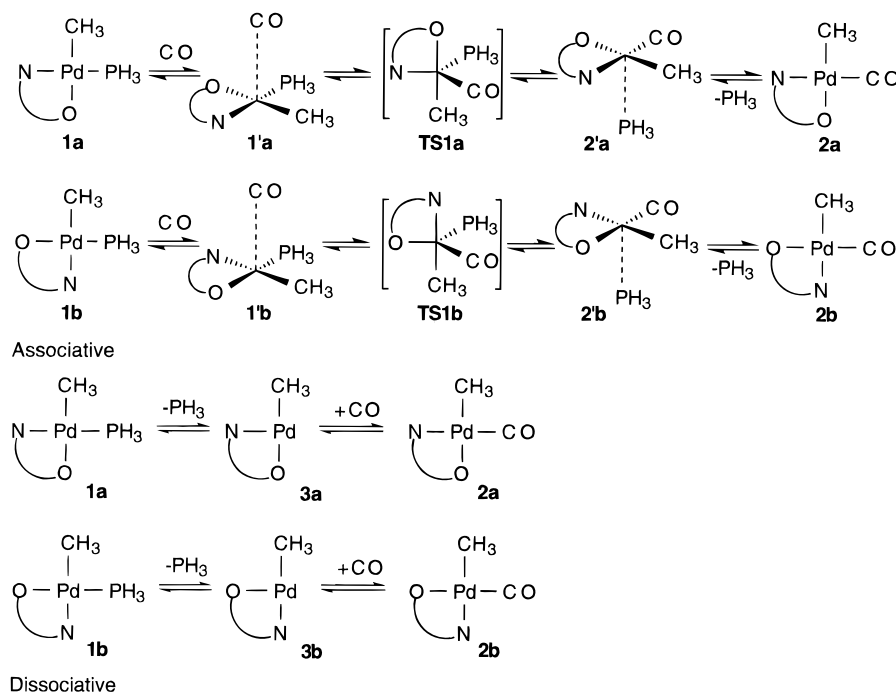


Figure 1. Replacement of the phosphine ligand in **1a** and **1b** by carbon monoxide.¹⁸

Table 1. Metal–Ligand Bond Lengths of the Reactants, Intermediates, and Transition Structures Involved in the Replacement of Phosphine with Carbon Monoxide, Calculated at B-LYP/[basis set A]^a

| structure | bond lengths (Å) | | | | |
|------------------------|--------------------|---------------|---------------|---------------|--------------------|
| | Pd–PH ₃ | Pd–CO | Pd–N | Pd–O | Pd–CH ₃ |
| 1a | 2.274 (2.261) | | 2.107 (2.101) | 2.174 (2.139) | 2.088 (2.051) |
| 1b | 2.276 (2.265) | | 2.213 (2.211) | 2.109 (2.073) | 2.074 (2.048) |
| 1'a | 2.281 (2.259) | 3.025 (3.082) | 2.110 (2.102) | 2.179 (2.144) | 2.088 (2.051) |
| 1'b^b | (2.254) | (3.012) | (2.197) | (2.082) | (2.055) |
| TS1a | 2.322 (2.271) | 2.157 (2.174) | 2.249 (2.263) | 2.185 (2.153) | 2.104 (2.071) |
| TS1b | 2.370 (2.288) | 2.106 (2.123) | 2.209 (2.201) | 2.221 (2.200) | 2.100 (2.080) |
| 2'a^b | (3.289) | (1.855) | (2.107) | (2.150) | (2.067) |
| 2'b^b | (3.368) | (1.841) | (2.202) | (2.077) | (2.073) |
| 2a | | 1.891 (1.860) | 2.105 (2.095) | 2.174 (2.133) | 2.102 (2.068) |
| 2b | | 1.886 | 2.220 | 2.082 | 2.091 |
| 3a | | | 2.015 | 2.167 | 2.048 |
| 3b | | | 2.203 | 2.071 | 2.024 |

^a The results for both isomers are included. Parameters calculated at MP2/[basis set A] are in parentheses. ^b Corresponding structures could not be located at B-LYP/[basis set A], as discussed previously.¹⁸

RECP and basis set will be referred to as “basis set A”. These levels of theory have been shown to give reasonable geometries for these complexes.¹⁸

For the density functional calculations, nonlocal corrections were included using Becke’s 1988 exchange functional²⁷ with the correlation functional of Lee, Yang, and Parr²⁸ (denoted B-LYP). An unpruned fine (75 302) grid was employed for integration (75 radial shells around each atom and 302 angular points in each shell). As energies generated by density functional methods appear to be unreliable for these systems,^{18,29} single-point energy calculations were performed at the MP2 level of theory using the B-LYP geometries with the same RECP and basis set. The core electrons were frozen in all MP2 calculations.

For further refined energies, single-point MP2 calculations were performed employing the LANL2 RECP with the (9s/6p/5d/4f)/[33111/3111/2111/211] valence basis set of Bauschlicher *et al.*³⁰ and 6-311+G(2d,p) on the main group elements. This

basis set will be denoted “basis set B”. For single-point calculations, “//” will be used to mean “at the structure optimized with”.

*C*_s symmetry was adopted for the four-coordinate reactants, the first four-coordinate intermediates (**2a** and **2b** in Figure 1), and the three-coordinate intermediates (**3a** and **3b** in Figure 1). *C*₁ symmetry was used for all other intermediates and transition structures.

Results and Discussion

The main results for the correlated calculations are presented in Tables 1–5. MP2 geometry optimizations have been performed for the key transformations of the competitive pathways. In the majority of cases there is excellent agreement between the energies determined at the MP2 level with the MP2 or B-LYP geometries. Where this agreement deviates, the apparent contradiction can be attributed to differences in geometry and becomes more pronounced for the single-point MP2 calculations employing basis set B. It is worth noting that, while the energies of the five-coordinate species with respect to the four-coordinate intermediates are

(27) Becke, A. D. *Phys. Rev. A* **1988**, *38*, 3098.

(28) Lee, C.; Yang, W.; Parr, R. G. *Phys. Rev. B* **1988**, *37*, 785.

(29) Frankcombe, K. E.; Cavell, K. J.; Yates, B. F.; Knott, R. B. *J. Phys. Chem.* **1995**, *99*, 14316.

(30) Langhoff, S. R.; Petterson, L. G.; Bauschlicher, C. W., Jr.; Partridge, H. J. *J. Chem. Phys.* **1987**, *86*, 268.

Table 2. Relative Energies of the Reactants, Intermediates, and Transition Structures Involved in Transformations Prior to Methyl Migration (kJ/mol)

| | energies; geometries | | | | |
|------------------------|---------------------------------|-------------------------------|-----------------------------|-------------------------------|-----------------------------|
| | B-LYP/basis A; B-LYP/basis A | MP2/basis A; B-LYP/basis A | MP2/basis A; MP2/basis A | MP2/basis B; B-LYP/basis A | MP2/basis B; MP2/basis A |
| 1a | 0 | 0 | 0 | 0 | 0 |
| 1b | 2.33 | 1.3 | 1.6 | -0.6 | +0.9 |
| 1'a | -3.0 | -6.2 | -9.3 | -14.2 | -18.8 |
| 1'b^a | | | -10.2 | | -20.4 |
| TS1a | 7.9 | 18.7 | 15.0 | 1.2 | -4.5 |
| TS1b | 18.6 | 27.3 | 23.0 | 6.3 | -4.9 |
| 2'a^a | | | -10.2 | | -22.2 |
| 2'b^a | | | -23.6 | | -38.8 |
| 2a | -36.9 | 6.5 | 5.1 | 6.9 | 4.1 |
| 2b | -44.9 | -7.9 | | -11.9 | |
| 3a | 132.4 | 171.0 | | 238.5 | |
| 3b | 124.6 | 169.1 | | 232.4 | |
| TS2 | -2.1 | 7.9 | 3.1 | 0.1 | -9.0 |
| TS3 | 9.25 | 17.6 | 14.7 | 6.3 | 2.4 |
| 4c | -18.5 | -14.5 | -23.0 | -36.1 | -52.7 |
| TS4 | -1.4 | 7.5 | | -15.2 | |
| 4 | -35.9 | -23.1 | -23.3 | -44.0 | -46.4 |

^a Corresponding structures could not be located at B-LYP/[basis set A].

Table 3. Selected Bond Lengths (Å) and Bond Angles (deg) of the Species Involved in the Replacement of the Donor Nitrogen by the Phosphine Ligand at B-LYP/[basis set A]^a

| | TS2 | TS3 | 4' | TS4 | 4 |
|-----------------------|---------------|---------------|---------------|------------|---------------|
| Pd-PH ₃ | 2.863 (2.746) | 2.810 (2.747) | 2.514 (2.482) | 2.526 | 2.516 (2.491) |
| Pd-CO | 1.881 (1.833) | 1.885 (1.847) | 1.887 (1.827) | 1.882 | 1.888 (1.850) |
| Pd-CH ₃ | 2.115 (2.106) | 2.120 (2.093) | 2.120 (2.089) | 2.120 | 2.124 (2.095) |
| Pd-O | 2.094 (2.096) | 2.482 (2.357) | 2.127 (2.191) | 2.073 | 2.080 (2.057) |
| Pd-N | 2.535 (2.407) | 2.120 (2.115) | 2.722 (2.351) | 3.615 | 4.848 (4.789) |
| CO-Pd-CH ₃ | 89.4 (83.6) | 90.8 (84.8) | 87.7 (84.9) | 88.0 | 88.9 (86.0) |

^a MP2/[basis set A] parameters are in parentheses.

Table 4. Selected Geometrical Parameters of the Methyl Migration Transition Structures and Products at B-LYP/[basis set A]^a

| | bond lengths (Å) | | | | | angle (deg) |
|-------------------------|--------------------|---------------|--------------------|---------------|---------------------------|-------------|
| | Pd-CH ₃ | Pd-CO | Pd-PH ₃ | Pd-N | Pd-O | C-Pd-C |
| TS5 | 2.363 (2.275) | 1.875 (1.828) | 2.372 (2.389) | | 2.130/3.265 (2.129/3.225) | 54.7 (54.3) |
| TS6 | 2.334 (2.274) | 1.868 (1.807) | 2.354 (2.363) | 2.563 (2.385) | 2.182 (2.210) | 54.7 (53.3) |
| TS7a^b | (2.276) | (1.805) | (2.732) | (2.269) | (2.146) | (51.7) |
| TS7b^b | (2.272) | (1.801) | (2.701) | (2.155) | (2.221) | (52.1) |
| TS8a | 2.358 | 1.863 | | 2.208 | 2.111 | 51.1 |
| TS8b | 2.341 | 1.869 | | 2.104 | 2.157 | 50.1 |
| 5a | | 2.044 (1.969) | 2.321 (2.293) | 2.106 (2.129) | 2.206 (2.179) | |
| 5b | | 2.033 | 2.320 | 2.293 | 2.133 | |
| 6 | | 2.013 | 2.313 | | 2.178/2.362 | |
| 7a | 2.562 | 1.916 | | 2.255 | 2.114 | 38.0 |
| 7b | 2.536 | 1.916 | | 2.088 | 2.191 | 38.5 |

^a MP2/[basis set A] values are in parentheses. ^b Corresponding structures could not be located at B-LYP/[basis set A].

poorly estimated at MP2/[basis set B]//B-LYP/[basis set A], energies relative to species of the same coordination number are close to those based on the MP2 geometries. Unless otherwise stated, in the following discussion the geometries and energetics were determined at MP2/[basis set A] and MP2/[basis set B]//MP2/[basis set A], respectively, and relative energies have been determined with respect to **1a** + CO. The complete PES at MP2/[basis set B]//MP2/[basis set A] for the lowest energy reaction pathway is depicted in Figure 2.

We have identified four possible reaction mechanisms for carbonylation in which alkyl migration is the rate-determining step. In the first section, we will discuss the possible ligand substitution and isomerization steps which may occur prior to methyl migration. In the second section, we will present a comparison of the possible methyl migration paths and an overview of the entire pathway. Experimentally, the reaction is carried

out in chloroform, which is generally regarded as a noncoordinating solvent. Preliminary calculations introducing a single solvent molecule at the RHF level with a large-core RECP²⁵ and a minimal basis set indicated that discrete solvent-solute interactions would not significantly influence the reaction pathway.³¹

1. Ligand Substitution Reactions and Isomerization. 1.1. Replacement of the Phosphine Ligand by Carbon Monoxide. Here, we extend our previous investigation of the ligand substitution reaction of **1a**¹⁸ to include the corresponding associative mechanism of the *cis*(N,P) isomer, **1b**, and the dissociative mechanism for both isomers (Figure 1). The metal-ligand bond lengths and relative energies of the species involved in the associative and dissociative mechanism are displayed in Tables 1 and 2, respectively.

(31) Frankcombe, K. E.; Yates, B. F. unpublished work.

Table 5. Relative Energies of the Transition Structures and Products of the Migration Steps (kJ/mol)

| | energies; geometries | | | | | migration |
|-------------------------|---------------------------------|-------------------------------|-----------------------------|-------------------------------|-----------------------------|-----------|
| | B-LYP/basis A; B-LYP/basis A | MP2/basis A; B-LYP/basis A | MP2/basis A; MP2/basis A | MP2/basis B; B-LYP/basis A | MP2/basis B; MP2/basis A | |
| TS5 | +28.2 | +43.1 | +42.1 | +25.4 | +24.8 | A |
| TS6 | +30.9 | +38.3 | +30.9 | +19.5 | +6.0 | B |
| TS7a^a | | | +58.5 | | +56.0 | C |
| TS7b^a | | | +43.9 | | +35.3 | D |
| TS8a | +34.0 | +83.6 | | +101.6 | | E |
| TS8b | +29.1 | +73.0 | | +84.9 | | F |
| 5a | -79.0 | -41.9 | -51.6 | -40.0 | -59.7 | |
| 5b | -88.8 | -63.5 | | -57.1 | | |
| 6 | -65.8 | -29.9 | | -15.3 | | |
| 7a | +18.7 | +96.7 ^b | | | | |
| 7b | +18.7 | +77.1 ^b | | | | |

^a Corresponding structures could not be located at B-LYP/[basis set A]. ^b Note that the single-point MP2 energies for these intermediates are higher than the single point energies of the transition structures corresponding to their formation (**TS8a** and **TS8b** for **7a** and **7b**, respectively). As single-point MP2 calculations using [basis set B] appear not to significantly vary the relative energy of four-coordinate structures, such calculations were not performed on **7a** and **7b**.

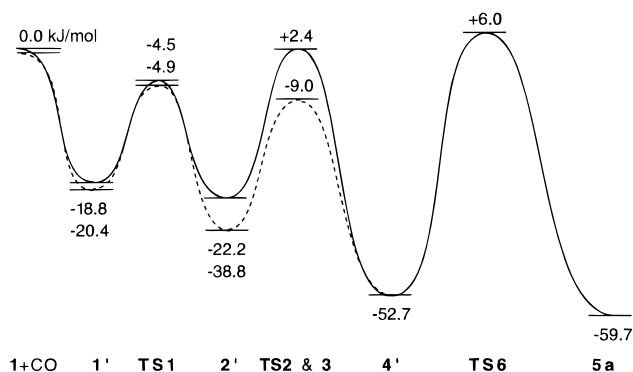


Figure 2. Potential energy surface for the lowest energy pathway (via Migration B, **TS6**) at MP2/[basis set B]/MP2-[basis set A].

Irrespective of the level of theory used, there was found to be less than 3 kJ/mol difference in energy between the two isomers **1a** and **1b**. This is consistent with the experimental observation that the initial complex (**I**) is obtained as an isomeric mixture.^{16,17} The associative ligand substitution of **1b** is similar to that of **1a**, proceeding via a trigonal-bipyramidal transition structure (**TS1b** in Figure 1) with a barrier of +15.5 kJ/mol with respect to the preceding intermediate, **1'b**.

In the absence of solvent effects, it is clear from the energies given in Table 2 that the dissociative mechanism is unfavorable. Expansion of the basis set at the MP2 level decreased the possibility of a competitive dissociative mechanism, generating a reaction barrier of +232.4 kJ/mol. The effect of increasing the basis set size can, thus, be summarized as follows: the relative energy of the five-coordinate species decreases, the stability of four-coordinate intermediates does not vary greatly, and three-coordinate species become less stable.

A search for a transition structure corresponding to replacement of the donor nitrogen by carbon monoxide was unsuccessful. The calculations are, therefore, consistent with experimental results. Replacement of triphenylphosphine in **I** with the less labile (but stronger *trans* influencing) tricyclohexylphosphine inhibits carbonylation.¹⁶ This indicates that partial or full dissociation of the phosphine must take place.

1.2. Replacement of the Donor Nitrogen by the Phosphine for 2'b. The substitution is illustrated in Figure 3. Tables 2 and 3 display the geometries and energies of the intermediates and transition structures

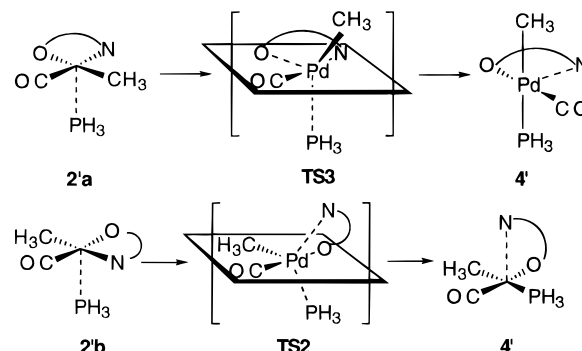


Figure 3. Replacement of the donor nitrogen by the phosphine ligand, incorporating isomerization for **2'a**.

involved. As for the substitution of PH_3 by CO, the reaction proceeds via a five-coordinate pseudo trigonal-bipyramidal transition structure (**TS2** in Figure 3) in which the nitrogen, phosphine, and methyl groups occupy positions in the equatorial plane. The activation energy was calculated to be 29.8 kJ/mol with respect to **2'b**, higher than the activation energy for the substitution of PH_3 by CO (14.3 and 15.5 kJ/mol from intermediates **1'a** and **1'b**, respectively). Refer to Figure 2, which includes these steps as part of the complete PES.

The product of this step is of particular interest (**4'** in Figures 3 and 4). In contrast to previous five-coordinate intermediates which have been challenging for density functional methods, the B-LYP functional located an intermediate in which the nitrogen–metal bond was lengthened from a typical equilibrium value of 2.1–2.2 to 2.722 Å. Refinement of the geometry at MP2/[basis set A] generated a strengthened Pd–N bond of 2.351 Å. The geometry of the intermediate closely resembles the crystal structures of similar five-coordinate platinum intermediates incorporating bidentate ligands obtained by Pacchioni and co-workers.³² Furthermore, this is the first theoretical investigation of the carbonylation of square-planar palladium(II) complexes in which a *strongly* bound five-coordinate intermediate has been located. Markies *et al.*¹⁵ located a neutral intermediate in which a NH_3 group was weakly associated to the metal with a bond length of 3.11 Å, which is most likely an artifact of BSSE. The stronger bond in the present study may be a result of ligands

(32) Fanizzi, F. P.; Maresca, L.; Natile, G.; Lanfranchi, M.; Tiripicchio, A.; Pacchioni, G. *J. Chem. Soc., Chem. Commun.* **1992**, 333.

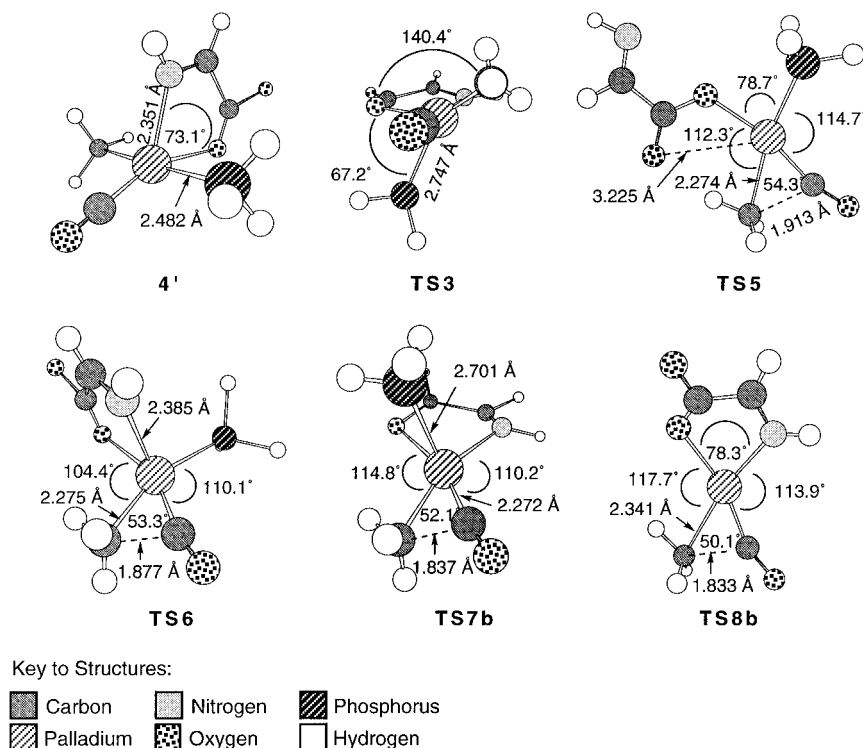


Figure 4. Selected structures optimized at MP2/[basis set A], with the exception of **TS8b** which was optimized at B-LYP/[basis set A].

with increased π back-donating ability or the inclusion of electron correlation in the geometry optimizations. Large basis set single-point calculations reinforce the stability of this intermediate, yielding an energy relative to **1a** + CO of -52.7 kJ/mol.

Two transformations from **4'** have been considered: methyl migration directly from **4'** *via* migration B and full dissociation of the nitrogen prior to migration *via* migration A (refer to Figure 5). A modest barrier of $+20.9$ kJ/mol at MP2/[basis set B]/B-LYP/[basis set A] was found to be associated with the dissociation of the donor nitrogen relative to **4'**. The transition structure for this transformation (**TS4**) was unremarkable, resembling **4'** with an elongated Pd–N distance of 3.615 Å. There is little difference in energy between the intermediates in which the nitrogen was weakly bound (**4'**) and unbound (**4**) (Table 2). Hence, whether migration occurs from **4'** or **4** in this case may depend on the relative barriers and reaction energies for methyl migration.

1.3. Ligand Substitution and Isomerization of 2'a. The geometries and energies of the transition structure and intermediates involved are given in Tables 2 and 3, respectively. The transformation is illustrated in Figure 3. It was surprising that the relative energy of **5a** is higher than that of **5b** by 17.1 kJ/mol (at MP2/[basis set B]/B-LYP/[basis set A]), and yet experimentally only the *trans*(N,P) isomer is observed.^{16,17} This indicates a number of possibilities, the most likely of which is that the *trans*(N,P) product is formed and isomerization between the two isomers is not facile. As NMR studies of the experimental product demonstrate that isomerization is not facile and previous work has indicated that to promote methyl migration the highly *trans* influencing phosphine should be *trans* to the methyl group, the weight of the available

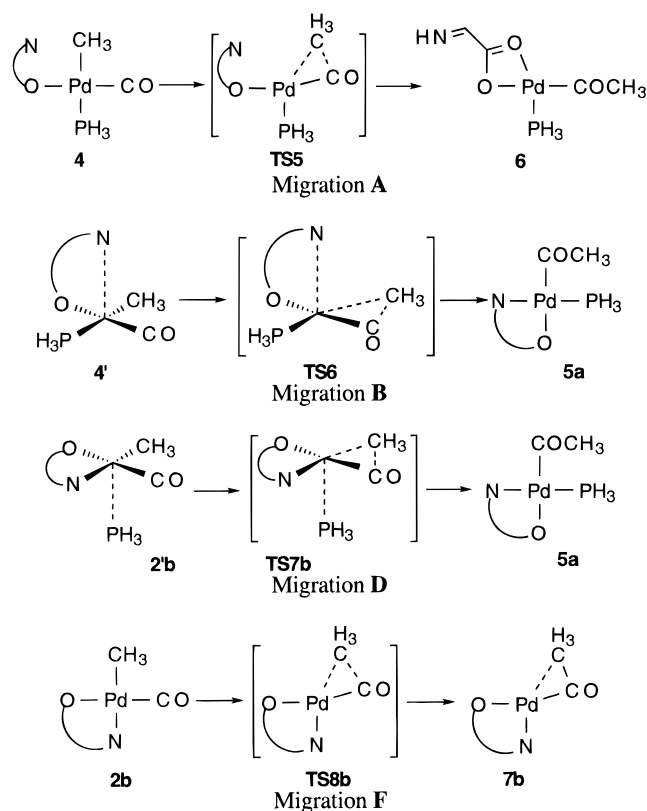


Figure 5. Methyl migration pathways.

evidence strongly supports that possibility. In this case isomerization must occur *prior* to methyl migration.

The well-known Berry pseudorotations cannot account for the isomerization of d^8 complexes unless there is a significant distortion of the flattened square-pyramidal geometry, typical of pentacoordinate pal-

ladium and platinum complexes, to an elevated square-pyramidal geometry prior to isomerization.³³ We have proposed³⁴ a novel pathway for isomerization with concomitant ligand substitution *via* the distorted transition structure (**TS3**) illustrated in Figures 3 and 4. Essentially, the methyl group moves out of the plane of the flattened square-pyramidal intermediate **2'a** toward a position *trans* to the phosphine. This causes a lengthening in the relatively strong palladium–oxygen bond, a result which provides the driving force for isomerization. In a single step, the carbonyl group moves to a position *trans* to the oxygen, transferring the elongation from the metal–oxygen to the more labile metal–nitrogen bond, and the metal–phosphine bond strengthens. The process occurs with a barrier of +24.6 kJ/mol relative to **2'a**. The resulting structure, **4'**, is identical to that obtained in the previous section for ligand substitution from **2'b** (Figure 3).

2. Methyl Migration. The geometries and relative energies of each of the species involved are displayed in Tables 4 and 5, respectively. We were unable to locate a transition structure which yielded a product consistent with a true carbonyl insertion process (i.e., one in which the resulting acyl group occupies the coordination position previously occupied by the methyl group).

It was previously suggested that methyl migration may proceed from a four-coordinate intermediate in which the donor nitrogen was unbound.¹⁶ We will refer to this path as migration A (Figure 5). The transition structure (**TS5** in Figures 4 and 5) for this process was found to be stabilized by a weak interaction between the metal and the carbonyl group of the bidentate ligand, such that the product of this step is the four-coordinate complex **6**. The activation energy for this step of the reaction was calculated to be +71.2 kJ/mol with respect to **4** (or +24.8 kJ/mol with respect to **1a** + CO). Two further transformations are required to generate the final product, **5a**.³⁵ It is, therefore, more likely that migration will take place from an intermediate in which the nitrogen is in a position to re-coordinate directly in the migration step.

Migration B refers to methyl migration from **4'** (Figure 5) in which the nitrogen recoordinates during the transformation to yield the *trans*(N,P) product, **5a**. The transition structure (**TS6** in Figures 4 and 5) is stabilized by the interaction between the metal and the donor nitrogen. Markies *et al.*¹⁵ observed a weaker stabilizing interaction for the cationic species $[\text{Pd}(\text{NH}_3)_2(\text{CH}_3)(\text{CO})\cdots(\text{NH}_3)]^+$; however, no stabilization was observed for their neutral model. The activation energy for migration B is +58.7 kJ/mol with respect to **4'** (or +6.0 kJ/mol with respect to **1a** + CO). The full PES for this mechanism is given in Figure 2, which is in excellent qualitative agreement with our PES previously presented employing medium basis sets.³⁴

Migrations C and D take place from the intermediates incorporating weakly bound phosphines (**2'a** and **2'b**, respectively). Migration D and the corresponding transition structure (**TS7b**) are illustrated in Figures 5 and 4, respectively. As these structures could not be suc-

cessfully treated using DFT, geometries were optimized only at the MP2 level. The transition structures are five-coordinate with methyl migration occurring concomitantly with the phosphine ligand re-establishing a normal coordination (**TS7a** and **TS7b** for migrations C and D, respectively). Migration D produces the correct *trans*(N,P) acyl product (**5a**). This process has an energy of +35.3 kJ/mol with respect to **1a** + CO. Conversely, migration C yields the *cis*(N,P) product (**5b**), which is not observed experimentally. The higher activation energy of migration C (+56.0 kJ/mol) compared to migration D is, therefore, consistent with experimental observations that only **5a** is formed.

Migrations E and F take place from the four-coordinate intermediates **2a** and **2b**, respectively, where the phosphine ligand has completely dissociated. Migration F is illustrated in Figure 5. In this case, the transition structures are four-coordinate (**TS8a** and **TS8b** for migrations E and F, respectively, the latter is depicted in Figure 4). The resulting intermediates (**7a** and **7b**) are pseudo four-coordinate, as the palladium–methyl bond does not fully break; instead, the methyl group attempts to accommodate the vacant coordination site prior to recoordination of the phosphine. This agostic interaction was only observed at the B-LYP level and provides minimal stabilization, hence, activating the C–C bond toward the reverse reaction. Note also that the barrier of migration E is higher than the barrier of migration F by 10.6 kJ/mol at MP2/[basis set A]/B-LYP[basis set A], *the latter migration yielding the correct product isomer*. The activation energies of these transformations are more than 29 kJ/mol higher than those of migrations A, B, and D, a difference which solvent effects are unlikely to offset. We can, therefore, conclude that the transition structure for methyl migration must be stabilized by an “incoming” fifth ligand, such that the product is truly four-coordinate.

Comparing all of these mechanisms, we observe little difference between the energies for migrations A, B, and D employing basis set A (Table 5). In fact, in the absence of more rigorous calculations we may be tempted to predict that migration D would be favorable due to the lower number of transformations involved. The importance of increasing the flexibility of the basis set is therefore clear. With basis set B, migration D is significantly less favorable than migrations A and B, indicating that migration proceeds *via* either partial or full dissociation of the donor nitrogen. The lower activation energy of migration B compared to migration A, coupled with the direct formation of the final product, **5a**, indicates that the former migration pathway will be preferred.

Our previous work suggests that the errors arising from an incomplete inclusion of electron correlation for the present system are in the range of 5–8 kJ/mol,¹⁸ so that we do not expect such errors to vary the qualitative conclusions of this work. More important are the consequences of employing PH₃ as a model for triphenylphosphine.^{19,20} The weaker π -accepting ability and larger steric bulk of triphenylphosphine would result in a destabilization of the five-coordinate relative to the four-coordinate species,^{32,33,36} and this issue requires further attention.

(33) der Heyde, T. A. *Angew. Chem., Int. Ed. Engl.* **1994**, *33*, 823.

(34) Frankcombe, K. E.; Cavell, K. J.; Knott, R. B.; Yates, B. F. *J. Chem. Soc., Chem. Commun.* **1996**, 781.

(35) Optimization of a transition structure for these transformations at a correlated level was not straight-forward.

(36) Albano, V. G.; Castellari, C.; Cucciolito, M. E.; Panunzi, A.; Vitagliano, A. *Organometallics* **1990**, *9*, 1269.

Conclusions

The present work has identified the lowest energy pathway for the carbonylation of the model system Pd(CH₃)(PH₃)(N-O) (Figure 2). The rate-determining step is methyl migration, the transition structure for which is stabilized by the approach of the partially dissociated donor nitrogen, thus producing a four-coordinate product. The reaction proceeds *via* a modest barrier and is exothermic overall. The lowest-energy pathway reflects well the experimentally found importance of the lability and *trans* influence of the phosphine ligand and the lability of the palladium–nitrogen bond. In addition, isomerization has been shown to occur prior to migration such that only the product isolated experimentally is obtained. Extending our conclusions to the experimental system (**I**), it is possible that the additional steric

bulk and reduced π -accepting ability of triphenylphosphine will favor the full dissociation of the donor nitrogen.

Finally, investigation of the dissociative ligand exchange mechanism indicates that the commonly discussed intermediates possessing a vacant coordination site (three-coordinate)^{4,16} are not energetically feasible.

Acknowledgment. The authors thank the Australian Research Council (ARC) and the Australian Institute of Nuclear Science and Engineering (AINSE) for their financial support of this project. They are also grateful to Dr. George Britosvek for a careful reading of the manuscript.

OM970063Z